

# Internucleosomal DNA cleavage in apoptotic WEHI 231 cells is mediated by a chymotrypsin-like protease

Jernej Murn<sup>1</sup>, Uros Urleb<sup>1,2</sup> and Irena Mlinaric-Rascan<sup>1,\*</sup>

<sup>1</sup>Faculty of Pharmacy, University of Ljubljana, Askerceva 7, 1000 Ljubljana, Slovenia

<sup>2</sup>Lek Pharmaceuticals d.d., Drug Discovery, Verovskova 57, Ljubljana, Slovenia

Although several lines of evidence support a role for serine proteases in apoptosis, little is known about the mechanisms involved. In the present study, we have examined the apoptosis-inducing potential and dissected the death-signalling pathways of N-tosyl-L-phenylalanine chloromethyl ketone (TPCK) and N-tosyl-L-lysine chloromethyl ketone (TLCK), inhibitors of chymotrypsin- and trypsin-like proteases, respectively. Our results designate two distinct roles for serine proteases. Firstly, we show that both inhibitors induce biochemical and morphological characteristics of apoptosis, including proteolysis of poly(ADP-ribose) polymerase 1 (PARP-1) and inhibitor of caspase-activated DNase (ICAD), as well as mitochondrial dysfunction, and that their action is abrogated by the caspase inhibitor benzyloxycarbonyl-Val-Ala-Asp.fluoromethylketone (z-VAD.fmk). These results suggest that inhibition of anti-apoptotic serine proteases governs the onset of the caspase-dependant apoptotic cascade. Secondly, we also demonstrate the involvement of a serine protease in the terminal stage of apoptosis. We showed that chymotrypsin-like protease activity is required for internucleosomal DNA fragmentation in apoptotic cells. Hence, DNA fragmentation is abrogated in TPCK-pre-treated WEHI 231 cells undergoing apoptosis triggered either by anti-IgM or TLCK. These results indicate that internucleosomal DNA cleavage in apoptotic cells is mediated by a chymotrypsin-like protease.

## Introduction

Apoptotic cells undergo a cascade of events characterized by distinct morphological changes, including plasma membrane blebbing, cell shrinkage, chromatin condensation, nuclear fragmentation and formation of apoptotic bodies. Two major pathways of apoptosis initiation have been described, the intrinsic and extrinsic pathways. The mechanisms involved in induction of apoptosis by chemotherapeutic agents such as alkylating substances, topoisomerase inhibitors and anti-mitotic agents are believed to be mediated predominantly by the intrinsic, mitochondrial pathway (Debatin *et al.* 2002; Ricci *et al.* 2003). The cell-suicide programme utilizes an evolutionarily conserved proteolytic cascade in which upstream (initiator) caspases mediate the activation of downstream (effector) caspases and numerous other cellular substrates (Hengartner 2000). Another prominent apoptotic

biochemical alteration is the increase in nuclease activity, resulting in chromatin degradation, a clearly irreversible lethal event. Cleavage of chromatin into oligonucleosomal fragments, which form the well-known apoptotic ladder, has been associated with several endonucleases, including CAD, endonuclease G, DNase I, and DNAS1L3 (Peitsch *et al.* 1993; Enari *et al.* 1998; Yakovlev *et al.* 1999; Li *et al.* 2001). However, the major endonuclease responsible for internucleosomal DNA cleavage during apoptosis is generally believed to be the caspase-activated DNase, CAD (Enari *et al.* 1998; Nagata 2000). CAD resides in the nucleus as an inactive heterodimer with its inhibitor ICAD (Widlak *et al.* 2003). Caspase-3, activated by apoptotic signals, cleaves ICAD to release CAD, which then degrades chromosomal DNA. Another caspase-3 substrate, poly(ADP-ribose) polymerase 1 (PARP-1), is an important DNA repair enzyme. Cleavage of PARP-1 during apoptosis has been thought to prevent futile repair of DNA strand breaks (Boulares *et al.* 2002).

Despite the widely accepted role of caspases in the cell-death programme, some caspase-deficient cells have been shown to undergo apoptosis normally in response

Communicated by: Tadashi Yamamoto

\*Correspondence: E-mail: irena.mlinaric@ffa.uni-lj.si

DOI: 10.1111/j.1365-2443.2004.00794.x

© Blackwell Publishing Limited

Genes to Cells (2004) 9, 1103–1111 **1103**

to various apoptotic stimuli, raising the possibility of functional redundancy of caspases in the system (Kuida *et al.* 1995; Hakem *et al.* 1998; Oppenheim *et al.* 2001). Indeed, activities of several proteases other than caspases have been implicated in apoptosis, for example papain-like lysosomal proteases (cathepsins) and the calcium-dependent cysteine protease, calpain (Ruiz-Vela *et al.* 1999; Mlinaric-Rascan & Turk 2003). Over the past few years, biochemical and genetic work has also identified a number of serine proteases that play important roles in the programmed disintegration of the cell (Stenson-Cox *et al.* 2003). One such example is a trypsin-like serine protease Omi/HtrA2, which can prevent XIAP inhibition of active caspase-3 and is able to counteract XIAP protection of mammalian NT2 cells against UV-induced cell death (Verhagen *et al.* 2002). The chymotryptic 24-kDa apoptotic protease (AP24) is another serine protease that is activated during apoptosis and has the ability to activate internucleosomal DNA fragmentation in various cell lines (Wright *et al.* 1994).

In this study, we have elucidated the molecular mechanism of cell death induced by inhibitors of serine proteases, chymotrypsin-like, TPCK and trypsin-like, TLCK. We show that this is a caspase-based process, which should render the DNase fully functional, however, only TLCK- but not TPCK-induced DNA laddering. These data suggest that TPCK interferes with the process of internucleosomal DNA cleavage.

## Results

### Inhibition of serine protease induces caspase activation and apoptosis

Inhibition of either chymotrypsin- or trypsin-like proteases induces apoptotic cell death, characterized by time-dependent caspase activation and degradation of specific substrates, ICAD and PARP-1. The kinetics of induction of cell death, monitored by Trypan Blue exclusion assay, differ between TPCK- and TLCK-treated cells. Incubation with 100  $\mu$ M TPCK or TLCK for 12 h killed 90% or 30% of cells, respectively (Fig. 1A). The inhibition of chymotryptic activity is reflected in a faster apoptotic response, than by the inhibition of tryptic activity. We assume this discrepancy to be because of either the biochemical or the pharmacological properties of the molecules, such as difference in affinity of inhibitors for their targets, the respective physiologic roles of proteases, cellular transport or metabolism.

Caspase activation was determined after incubating WEHI 231 cells with various concentrations of serine protease inhibitors. Firstly, cells were incubated with

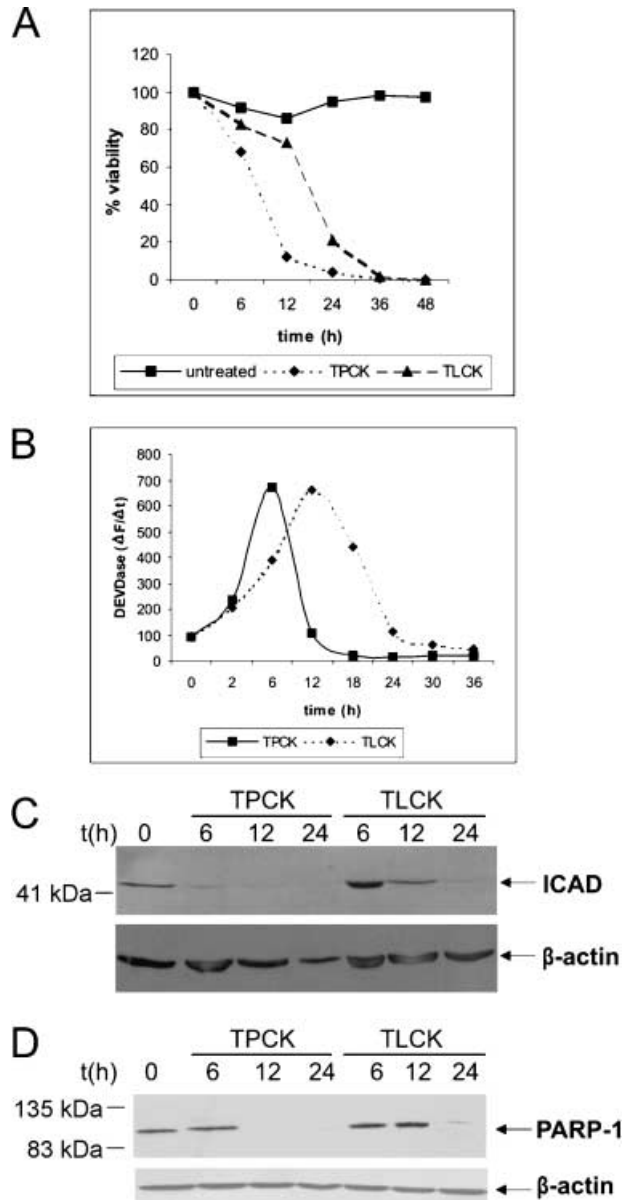


**Figure 1** Serine protease inhibitors TPCK and TLCK induce caspase activation and apoptosis. (A) Live cell count. Cells were treated with 100  $\mu$ M of TPCK or TLCK for the indicated time periods and viability was assessed by Trypan Blue staining. The data are mean values of three independent experiments. (B) Time-courses of DEVDase activity. Cells ( $2.5 \times 10^5$ /mL) were incubated with 100  $\mu$ M of TPCK or TLCK and harvested at the indicated times. Caspase/DEVDase activity was measured in whole cell lysates using Ac-DEVD.AFC substrate. The results are presented as changes in fluorescence as a function of time. (C) Anti-ICAD and (D) anti-PARP-1 immunoblots showing kinetics of ICAD and PARP-1 degradation in response to treatment of WEHI 231 cells with 100  $\mu$ M TPCK or TLCK. Equal amounts (40  $\mu$ g) of proteins were loaded for each line. Membranes were re-blotted with anti- $\beta$ -actin to confirm equal loading. The results are typical of at least three experiments.

TPCK (1, 10, 50 and 100  $\mu\text{M}$ ) for various periods of time, after which cell extracts were prepared and assayed for caspase-3-like activity with Ac-DEVD-AMC substrate. Concentrations of TPCK above 10  $\mu\text{M}$  induced a marked increase in DEVDase activity, which reached its peak at 6 h of incubation. Maximal DEVDase activity was observed in extracts of cells exposed to 100  $\mu\text{M}$  TPCK (Fig. 1B). In a similar experiment, treatment with the inhibitor of trypsin-like proteases TLCK (100  $\mu\text{M}$ ) resulted in a somewhat different profile of caspase activity that peaked at 12 h with a comparable intensity to that of TPCK at 6 h (Fig. 1B). These results clearly demonstrate a correlation between caspase activation and decrease in cell viability, indicating immediate cell death after the increases in DEVDase activity induced by both TPCK and TLCK. Similar results were also obtained with a human Burkitt's lymphoma cell line Raji, although with slower kinetics of caspase activation than observed in WEHI 231 cells (data not shown).

The functional activity of TPCK- and TLCK-induced DEVDase was examined by two caspase-3 substrates, PARP-1 and ICAD. WEHI 231 cells were treated with TPCK and TLCK for 6, 12 and 24 h and whole cell extracts screened by immunoblotting for the presence of intact ICAD and PARP-1. Both TPCK and TLCK induced time dependent cleavage of ICAD and PARP-1, which correlated well with the time course of caspase activation for both inhibitors. The intensity of the 45-kDa immunoreactive band corresponding to ICAD was significantly reduced on 6- and 12-h Western blots of extracts of TPCK-

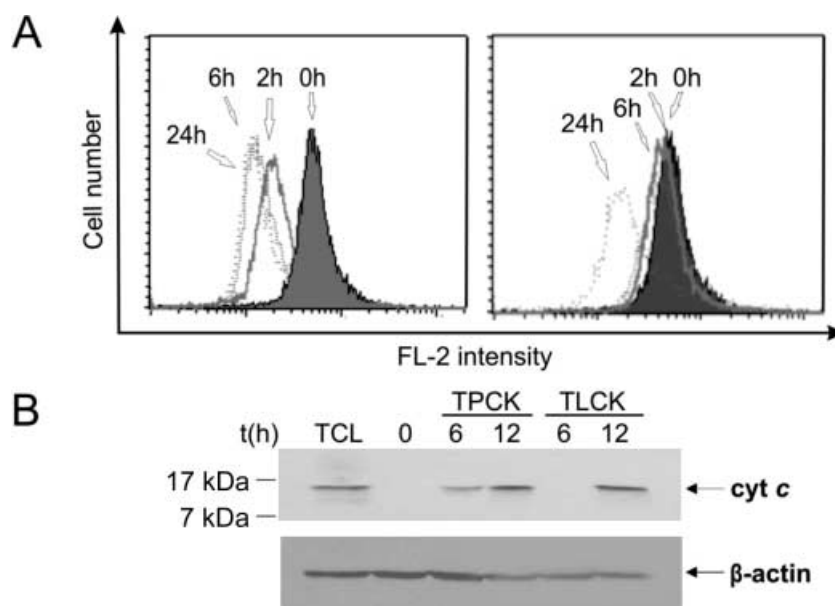
and TLCK-treated cells, respectively (Fig. 1C). Similarly, PARP-1 cleavage occurred in response to caspase activation (Fig. 1D). Immunoblotted PARP-1 was detected as a 118-kDa protein, which is cleaved by active caspase-3 into an 85-kDa fragment, which did not react with our N-terminus-recognizing antibody.

These findings suggest that the inhibition of either chymotrypsin- or trypsin-like proteases induces apoptotic cell death.

### TPCK- or TLCK-induced apoptosis includes changes in mitochondrial membrane potential and permeability

Treatment of WEHI 231 cells with serine protease inhibitors led to loss of mitochondrial membrane potential ( $\Psi_m$ ) and the release of cytochrome *c*. Staining cells with mitochondria-sensitive MitoTracker Red CMXRos dye, whose sequestration into mitochondria is sensitive to transmembrane potential, revealed a significant and time-dependent drop in fluorescence intensity in cells exposed to the inhibitors, compared with untreated cultures. Flow cytometry analysis showed that treatment of cells with TPCK induced changes in  $\Psi_m$ , which could be detected at 2 h, and the red fluorescence continued to fade until 6 h of incubation (Fig. 2A, left panel). In a similar experiment, loss of  $\Psi_m$  was observed only after 24 h of exposure to TLCK (Fig. 2A, right panel). Changes in  $\Psi_m$  corresponded temporally to other biochemical and morphological alterations for both TPCK and TLCK.

**Figure 2** TPCK- and TLCK-induced mitochondrial depolarization and cytochrome *c* release. (A) WEHI 231 cells were treated with 100  $\mu\text{M}$  TPCK (left panel) or 100  $\mu\text{M}$  TLCK (right panel) for the indicated time periods, and incubated with MitoTracker Red CMXRos for the last 30 min. Changes in  $\Psi_m$  were measured by cells' differential uptake of MitoTracker dye. Representative flow cytometry histograms are shown. (B) Western blot analysis of mitochondrial cytochrome *c* release. WEHI 231 cells were treated with 100  $\mu\text{M}$  TPCK or TLCK for the indicated time periods. Cytosolic fractions were prepared by selective plasma membrane permeabilization with digitonin and submitted for immunoblot analysis. Equal amounts of proteins (40  $\mu\text{g}$ ) were loaded per well. Membrane was re-blotted with anti- $\beta$ -actin to confirm equal loading. The results are typical of at least three experiments. Total cell lysate of untreated cells (TCL) was used as a positive control.



Concomitant release of cytochrome *c* from mitochondria into the cytosol confirmed changes in mitochondrial membrane permeability (MMP). The cytosolic fractions of WEHI 231 cells incubated with or without TPCK or TLCK were prepared by selective plasma membrane permeabilization with digitonin. Analysis of these fractions by immunoblotting showed that, while cytochrome *c* was confined to mitochondria in normally proliferating cells, both TPCK and TLCK caused its leakage into the cytosol in a time-dependent manner, contributing to mitochondria-mediated apoptosis (Fig. 2B). The above results show that the increase in MMP corresponds to the loss of  $\Psi_m$  in TPCK- or TLCK-induced apoptosis.

#### Chymotryptic activity interferes with internucleosomal DNA cleavage

As both serine protease inhibitors induced apoptotic cell death and caspase activation, internucleosomal cleavage of DNA was also expected to occur. The integrity of genomic DNA was monitored over 48 h of incubation with increasing concentrations of either TPCK or TLCK or both. Surprisingly, agarose gel electrophoresis of the DNA from cells incubated with TPCK revealed a total absence of DNA laddering pattern, irrespective of the incubation time or TPCK concentration. In contrast, TLCK resulted in extensive internucleosomal cleavage, which was both time- and concentration-dependent. These changes were confirmed both by electrophoresis (Fig. 3A) and also by staining cellular DNA with propidium iodide followed by FACS analyses (data not shown). When both TPCK and TLCK were added to cells in culture at the same time, no laddering was observed, implying that TPCK acts as an inhibitor of DNase or the upper signalling molecule (Fig. 3B).

To elaborate the mechanism responsible for the differential effects of the two inhibitors on DNA fragmentation, we asked the question as to whether TPCK would interfere with internucleosomal DNA fragmentation in anti-IgM-treated WEHI 231 cells, which are known to undergo growth arrest and apoptosis on B cell antigen receptor (BCR) crosslinking. Cells were pre-incubated with 10  $\mu$ M TPCK or TLCK for 1 h prior to addition of anti-IgM antibodies, and harvested 12, 24 or 48 h later. Again, as shown in Fig. 3(C), TPCK completely inhibited BCR-mediated DNA laddering, while the addition of TLCK had no effect.

Therefore, despite the fact that both inhibitors caused liberation of CAD from its inhibitor ICAD (see Fig. 1C), which should render the DNase fully functional, only TLCK induced DNA laddering. These data suggest that TPCK interferes with the process of internucleosomal DNA cleavage downstream of CAD.

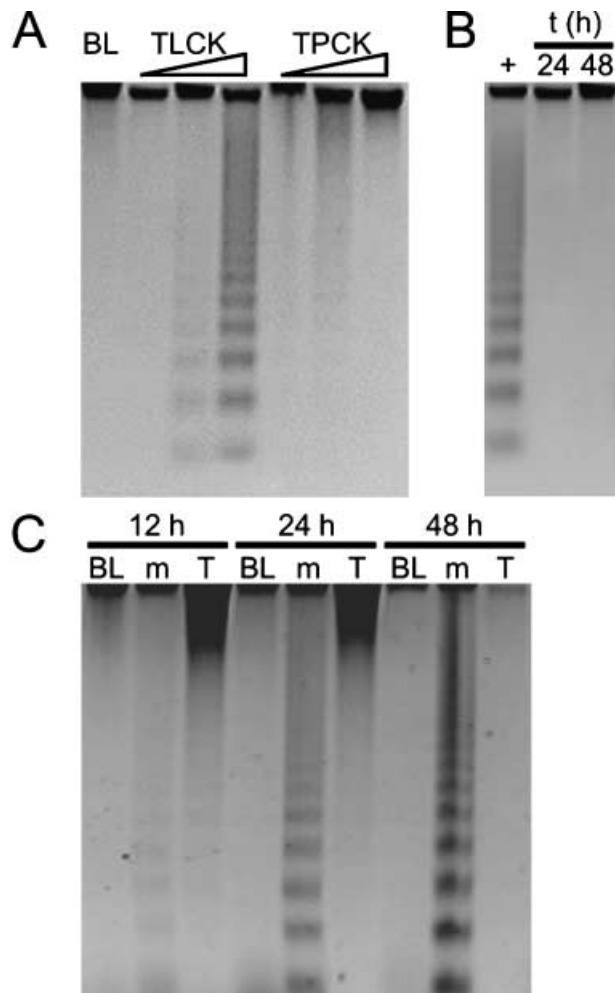


**Figure 3** TPCK interferes with DNA laddering. (A) Cells were incubated with 10, 50 and 100  $\mu$ M TLCK or TPCK for 24 h and the extracted DNA subjected to agarose gel electrophoresis. (B) Incubation of cells with a combination of TLCK (100  $\mu$ M) and TPCK (100  $\mu$ M) for 24 and 48 h. DNA of cells incubated with 100  $\mu$ M TLCK for 24 h was used as a positive control (+). (C) TPCK prevents BCR-mediated DNA laddering. WEHI 231 cells were incubated for the indicated periods of time with 10  $\mu$ g/mL of anti-IgM antibody with (T) or without (m) pre-incubation with 10  $\mu$ M TPCK for 30 min (control cells, BL). The extracted DNA was analysed by agarose gel electrophoresis.

#### TPCK- or TLCK-induced apoptotic changes are caspase dependent

Inhibition of serine proteases resulted in a significant elevation of caspase activity, caused damage to mitochondria and governed cell to apoptotic demise. We examined the interdependence of these events and found that serine proteases act downstream of caspases. Pre-incubation of



cells with 100  $\mu\text{M}$  z-VAD.fmk for 1 h totally suppressed the activity of caspases throughout the time-course of the experiment (data not shown). Caspase inhibition resulted in continued cell viability, as assessed by exclusion of Trypan Blue (data not shown).

The effects of caspase inhibition on biochemical and morphological changes induced by serine protease inhibitors were visualized using bright-field phase contrast and fluorescence microscopy. Morphologic examination revealed that, while untreated WEHI 231 cells were large (10–18  $\mu\text{m}$ ) with regular circular outline, treatment with 100  $\mu\text{M}$  TPCK or TLCK resulted in prominent membrane blebbing and cell shrinkage. These apoptotic changes were largely prevented by 100  $\mu\text{M}$  z-VAD.fmk, indicating that pre-treatment with the latter protected WEHI 231 cells against serine protease inhibitor-induced apoptosis (Fig. 4A). This conclusion is further supported by results indicating that inhibition of serine proteases induced marginalization and condensation of chromatin into numerous small clumps, which is in marked contrast with the uniform distribution of chromatin in the nuclei of untreated cells, as examined by labelling of DNA with selective Hoechst 33342 (Fig. 4B, left set of panels). At the same time, only mitochondria of untreated, but not TPCK- and TLCK-treated, cells exhibited intense MitoTracker staining (Fig. 4B, right set of panels). Again, in agreement with the above results, pre-incubation with z-VAD.fmk entirely preserved the activity of mitochondria under both TPCK- and TLCK-treatments (also confirmed by FACS analysis). We also examined whether oligonucleosomal DNA cleavage induced by 100  $\mu\text{M}$  TLCK is a caspase-dependent event. Pre-incubation of cells with z-VAD.fmk effectively prevented DNA laddering at all time intervals examined (Fig. 4C).

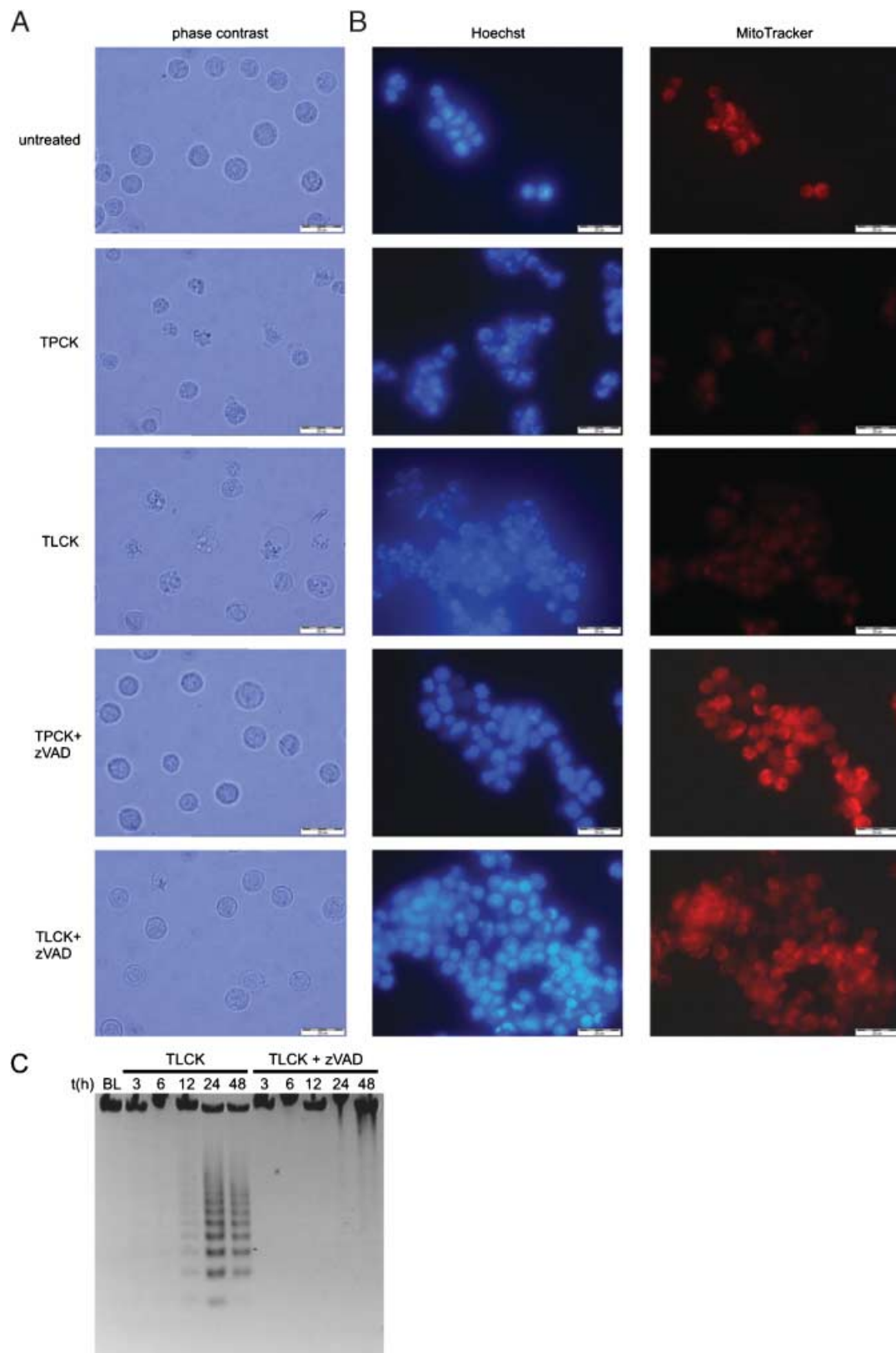
These observations demonstrate that serine proteases act downstream of caspases and therefore if caspases are inhibited, the cells are resistant to the action of protease inhibitors.

## Discussion

These results suggest at least two distinct roles for serine proteases, one being important for cell survival, the other facilitating internucleosomal DNA cleavage in apoptotic cells. We showed initially that inhibitors of both chymotrypsin and trypsin serine proteases, TPCK and TLCK, respectively, trigger cell death in a manner similar to many chemotherapeutic agents that induce apoptosis via mitochondrial apoptotic pathways (Debatin *et al.* 2002). Although inhibition of both classes of serine proteases resulted in a potent induction of mitochondrial dysfunction and apoptosis, the caspase inhibition effectively

blocked the development of morphological and biochemical apoptotic features, as well as death of WEHI 231 cells, implying that serine proteases act downstream of caspases. This crucial finding implies that cell death induced by the two inhibitors results from a coordinated sequence of events and precludes the possibility of necrotic cell demise that would follow as a consequence of non-specific alkylation. However, the primary target(s) of TPCK and TLCK that initiates the cell death programme is not known, but may involve anti-apoptotic serine proteases whose inhibition constitutes a death signal. Several other molecular mechanisms for TPCK- and TLCK-induced apoptosis have been proposed. For example, TPCK has been reported to induce p53-dependent activation of caspases-3 and -7 (Kim *et al.* 2003) and to promote apoptosis by inhibiting NF- $\kappa$ B/Rel binding (Wu *et al.* 1996a), decreasing *c-myc* expression (Wu *et al.* 1996b), and others (Biró *et al.* 1992; Drexler 1997).

Besides their role in the proximal stage of apoptosis, serine proteases are also involved in the process of internucleosomal DNA cleavage (Fig. 3A). In addition, lower concentrations of TPCK (5–10  $\mu\text{M}$ ), which did not affect cell viability, also prevented BCR-mediated DNA laddering in WEHI 231 cells. The lack of DNA laddering pattern in TPCK-triggered cell death has been observed in most of the cell lines studied (Weaver *et al.* 1993; Fearnhead *et al.* 1995; Ghibelli *et al.* 1995; Zhu *et al.* 1997; Kugawa *et al.* 1998; Stenson-Cox *et al.* 2003). TPCK therefore appears to selectively target a molecule responsible for internucleosomal DNA cleavage. We observed that both serine protease inhibitors activated CAD, which is generally considered to be the nuclease primarily responsible for large-scale (50–300 kbp) and internucleosomal (~200 bp) DNA fragmentation and for chromatin condensation. Because some or all of these nuclear apoptotic features, other than DNA laddering, have been observed in various TPCK-treated cells by us and others (Weaver *et al.* 1993; Fearnhead *et al.* 1995; Zhu *et al.* 1997), CAD does not appear to be targeted by TPCK, and neither are caspases, which have  $\text{IC}_{50}$  values for TPCK well above 100  $\mu\text{M}$  (Foghsgaard *et al.* 2001). We therefore conclude that CAD, despite its activation by caspases, is not responsible for DNA laddering in the apoptosis of WEHI 231 cells. Among other possible candidates involved in oligonucleosomal cleavage in WEHI 231 cells is the apoptotic protein AP24, a 24-kDa chymotrypsin-like cytosolic protease, whose inhibition by TPCK has previously been demonstrated (Wright *et al.* 1997). It has been suggested that, on activation via mitochondrial damage, AP24 transforms leucocyte elastase inhibitor (LEI) to endonuclease L-DNase II, which then



translocates to the nucleus and induces DNA degradation (Torriglia *et al.* 1998; Stenson-Cox *et al.* 2003). We are currently investigating this possibility.

In conclusion, our data demonstrate that inhibition of anti-apoptotic serine proteases induces caspase-dependent apoptotic cell death. Chymotryptic serine protease also acts in the terminal phase of apoptosis, where it interferes with the induction of internucleosomal DNA cleavage.

## Experimental procedures

### Cell culture and treatments

WEHI 231 cells were cultured in RPMI 1640 medium (Sigma, Chemical Co., St Louis, MO) supplemented with 10% foetal calf serum (Gibco, Grand Island, NY), 2 mM L-glutamine, 100 U/mL penicillin, 100 µg/mL streptomycin and 50 µM 2-mercaptoethanol (Sigma), at 37 °C, in humidified air with 5% CO<sub>2</sub>. Cell viability was assessed by Trypan Blue (Sigma) exclusion assay. Cells (10<sup>6</sup>/mL) were treated with TPCK, TLCK or goat anti-mouse IgM (Sigma), with or without pre-incubation with z-VAD.fmk (Bachem AG, Bubendorf, Switzerland) for 1 h. Appropriate volumes of the corresponding solvents were added to the control cultures.

### Assay of DEVDase activity

DEVDase activity was measured essentially as described (Mlinaric-Rascan & Turk 2003). Cell extracts (40 µg of protein) were incubated for 30 min at 37 °C with 100 µM Ac-DEVD.AFC peptide substrate (Bachem). The fluorescence of free 7-amino-4-trifluoromethyl coumarin (AFC), generated as a result of cleavage of the aspartate-AFC bond, was monitored continuously for 30 min with a fluorescence microplate reader (GENios SPEC-TRAFluor Plus, Tecan Systems Inc, San Jose, CA) at excitation and emission wavelengths of 405 and 535 nm, respectively. Assays performed without the cell lysate were used as background controls. Steady-state hydrolysis rates were obtained from the linear

part of the curves. Data were expressed as increase in fluorescence as a function of time ( $\Delta F/\Delta t$ ).

### Preparation of cytosolic extracts

Cytosolic fractions were generated using a digitonin-based subcellular fractionation technique as documented (Murphy *et al.* 2003). Cells were digitonin permeabilized for 5 min on ice at a density of  $3 \times 10^7$ /mL in cytosolic extraction buffer (250 mM sucrose, 70 mM KCl, 137 mM NaCl, 4.3 mM Na<sub>2</sub>HPO<sub>4</sub>, 1.4 mM KH<sub>2</sub>PO<sub>4</sub>, pH 7.2, 100 µM AEBSF, containing 250 µg/mL digitonin). Plasma membrane permeabilization of cells was confirmed by Trypan Blue staining. Cells were then centrifuged at 1000 *g* for 5 min at 4 °C. The supernatants (cytosolic fractions) were stored at -70 °C until use.

### Immunoblot analysis

Cell extracts were prepared by pelleting, lysing and sonicating cells in 0.1 M phosphate buffer pH 6.0 containing 0.1% Triton X-100 (Mlinaric-Rascan & Turk 2003). Each lysate (40 µg of protein) was fractionated by SDS-PAGE, transferred to PVDF membrane and probed with rabbit anti-ICAD (C-terminal, Sigma) or mouse anti-PARP-1 antibody (BD Biosciences, Pharmingen, San Diego, CA). Similarly, 40 µg of cytosolic proteins were probed with a mouse monoclonal antibody recognizing cytochrome *c* (BD Biosciences). Immune complexes were detected with either goat anti-rabbit IgG-AP (Southern Biotechnology Associates, Birmingham, LA) or peroxidase-coupled goat anti-mouse IgG (Upstate, Lake Placid, NY) and visualized using chromogenic (BCIP/NBT-PLUS Solution, Southern Biotechnology Associates) or chemiluminescence (Lumi GLO, Upstate) reagents, respectively. Blots were re-probed with anti-β-actin MAb (Sigma), to confirm equal loading.

### Analysis of internucleosomal DNA fragmentation

DNA was isolated from cells as previously described (Mlinaric-Rascan & Turk 2003) and electrophoresed through 1.8% agarose gels in Tris borate/EDTA buffer. The gels were stained with ethidium bromide.

### Flow cytometry analysis of mitochondrial membrane potential

The integrity of mitochondrial transmembrane potential was evaluated by staining cells with MitoTracker dye (MitoTracker Red CMXRos, Molecular Probes, Eugene, OR). Cells in culture ( $1 \times 10^6$ /mL) were incubated in the presence or absence of 100 µM TLCK or TPCK for designated time periods with 200 nM MitoTracker for the last 30 min of the incubation. They were then washed in fresh, pre-warmed growth medium, washed again in PBS, fixed in 4% paraformaldehyde and analysed by fluorescence-activated cell sorting (FACS Calibur, BD Biosciences, Immunocytometry Systems, San Jose, CA). Data were evaluated using the

**Figure 4** Caspase inhibition rescues cells from serine protease inhibitor-induced apoptosis. (A) and (B) WEHI 231 cells were treated with 100 µM TPCK or 100 µM TLCK for 24 h, with or without pre-incubation with 100 µM z-VAD.fmk for 1 h. (A) Representative bright-field phase contrast photomicrographs showing the absence of membrane blebbing and cell shrinkage in samples pre-treated with z-VAD.fmk. (B) Dual staining with Hoechst 33342 and MitoTracker Red CMXRos. Note the correlation between chromatin organization (Hoechst) and red staining of active mitochondria (MitoTracker). All bars = 20 µm (C) Oligonucleosomal DNA fragmentation is abolished in the absence of active caspases. Cells were pre-incubated with 100 µM z-VAD.fmk and treated with TLCK (100 µM) for the designated time intervals. Extracted DNA was subjected to agarose gel electrophoresis.

Cell-Quest software supplied by the manufacturer. The intensity of red fluorescence of the cells served as a measure of mitochondrial membrane potential.

## Fluorescence microscopy

For immunofluorescence, WEHI 231 cells were dually stained with MitoTracker and Hoechst 33342. Following staining of mitochondria and fixation as for flow cytometry analysis, cells were washed in PBS and permeabilized with 0.5% Triton X-100 for 10 min. They were then washed in PBS, stained with 20  $\mu$ M Hoechst 33342, washed again in PBS and mounted on polylysine-coated glass slides for visualization under fluorescence microscope (1000 $\times$  magnification; Olympus BX50, Olympus Optical Co., Hamburg, Germany).

## Acknowledgements

This work was supported in part by the Grant L1-5267-0787-03 from Slovenian Ministry of Education, Science, and Sports.

## References

- Biró, A., Sármay, G., Rozsnyay, Z., Klein, E. & Gergely, J. (1992) A trypsin-like serine protease activity on activated human B cells and various B cell lines. *Eur. J. Immunol.* **22**, 2547–2553.
- Boulares, A.H., Zoltoski, A.J., Contreras, F.J., Yakovlev, A.G., Yoshihara, K. & Smulson, M.E. (2002) Regulation of DNASE1L3 endonuclease activity by poly(ADP-ribosylation) during etoposide-induced apoptosis. *J. Biol. Chem.* **277**, 372–378.
- Debatin, K.M., Poncet, D. & Kroemer, G. (2002) Chemotherapy: targeting the mitochondrial cell death pathway. *Oncogene* **21**, 8786–8803.
- Drexler, H.C. (1997) Activation of the cell death program by inhibition of proteasome function. *Proc. Natl. Acad. Sci. USA* **94**, 855–860.
- Enari, M., Sakahira, H., Yokoyama, H., Okawa, K., Iwamatsu, A. & Nagata, S. (1998) A caspase-activated DNase that degrades DNA during apoptosis, and its inhibitor ICAD. *Nature* **391**, 43–50.
- Fearnhead, H.O., MacFarlane, M., Dinsdale, D. & Cohen, G.M. (1995) DNA degradation and proteolysis in thymocyte apoptosis. *Toxicol. Lett.* **82–83**, 135–141.
- Foghsgaard, L., Wissing, D., Mauch, D., *et al.* (2001) Cathepsin B acts as a dominant execution protease in tumor cell apoptosis induced by tumor necrosis factor. *J. Cell Biol.* **153**, 999–1009.
- Ghibelli, L., Maresca, V., Coppola, S. & Gualandi, G. (1995) Protease inhibitors block apoptosis at intermediate stages: a compared analysis of DNA fragmentation and apoptotic nuclear morphology. *FEBS Lett.* **377**, 9–14.
- Hakem, R., Hakem, A., Duncan, G.S., *et al.* (1998) Differential requirement for caspase 9 in apoptotic pathways *in vivo*. *Cell* **94**, 339–352.
- Hengartner, M.O. (2000) The biochemistry of apoptosis. *Nature* **407**, 770–776.
- Kim, K., Choi, K.H., Fu, Y.M., Meadows, G.G. & Joe, C.O. (2003) Dephosphorylation of p53 during cell death by N- $\alpha$ -tosyl-L-phenylalanyl chloromethyl ketone. *Biochem. Biophys. Res. Commun.* **306**, 954–958.
- Kugawa, F., Arae, K., Ueno, A. & Aoki, M. (1998) Buprenorphine hydrochloride induces apoptosis in NG108-15 nerve cells. *Eur. J. Pharmacol.* **347**, 105–112.
- Kuida, K., Lippke, J.A., Ku, G., *et al.* (1995) Altered cytokine export and apoptosis in mice deficient in interleukin-1 $\beta$  converting enzyme. *Science* **267**, 2000–2003.
- Li, L.Y., Luo, X. & Wang, X. (2001) Endonuclease G is an apoptotic DNase when released from mitochondria. *Nature* **412**, 95–99.
- Mlinaric-Rascan, I. & Turk, B. (2003) B cell receptor-mediated nuclear fragmentation proceeds in WEHI 231 cells in the absence of detectable DEVDase and FRase activity. *FEBS Lett.* **553**, 51–55.
- Murphy, B.M., O'Neill, A.J., Adrian, C., Watson, R.W.G. & Martin, S.J. (2003) The apoptosome pathway to caspase activation in primary human neutrophils exhibits dramatically reduced requirements for cytochrome *c*. *J. Exp. Med.* **197**, 625–632.
- Nagata, S. (2000) Apoptotic DNA fragmentation. *Exp. Cell Res.* **256**, 12–18.
- Oppenheim, R.W., Flavell, R.A., Vinsant, S., Prevette, D., Kuan, C.Y. & Rakic, P. (2001) Programmed cell death of developing mammalian neurons after genetic deletion of caspases. *J. Neurosci.* **21**, 4752–4760.
- Peitsch, M.C., Polzar, B., Stephan, H., *et al.* (1993) Characterization of the endogenous deoxyribonuclease involved in nuclear DNA degradation during apoptosis (programmed cell death). *EMBO J.* **12**, 371–377.
- Ricci, J.E., Waterhouse, N. & Green, D.R. (2003) Mitochondrial functions during cell death, a complex (I–V) dilemma. *Cell Death Diff.* **10**, 488–492.
- Ruiz-Vela, A., González de Buitrago, G. & Martínez-A, C. (1999) Implication of calpain in caspase activation during B cell clonal deletion. *EMBO J.* **18**, 4988–4998.
- Stenson-Cox, C., FitzGerald, U. & Samali, A. (2003) In the cut and thrust of apoptosis, serine proteases come of age. *Biochem. Pharmacol.* **66**, 1469–1474.
- Torriglia, A., Perani, P., Brossas, J.Y., *et al.* (1998) L-DNase II, a molecule that links proteases and endonucleases in apoptosis, derives from the ubiquitous serpin leukocyte elastase inhibitor. *Mol. Cell. Biol.* **18**, 3612–3619.
- Verhagen, A.M., Silke, J., Ekert, P.G., *et al.* (2002) HtrA2 promotes cell death through its serine protease activity and its ability to antagonize inhibitor of apoptosis proteins. *J. Biol. Chem.* **277**, 445–454.
- Weaver, V.M., Lach, B., Walker, P.R. & Sikorska, M. (1993) Role of proteolysis in apoptosis: involvement of serine proteases in internucleosomal DNA fragmentation in immature thymocytes. *Biochem. Cell Biol.* **71**, 488–500.
- Widlak, P., Lanuszewska, J., Cary, R.B. & Garrard, W.T. (2003) Subunit structures and stoichiometries of human DNA fragmentation factor proteins before and after induction of apoptosis. *J. Biol. Chem.* **278**, 26915–26922.



- Wright, S.C., Schellenberger, U., Wang, H., Kinder, D.H., Talhouk, J.W. & Larrick, J.W. (1997) Activation of CPP32-like protease is not sufficient to trigger apoptosis: inhibition of apoptosis by agents that suppress activation of AP24, but not CPP32-like activity. *J. Exp. Med.* **186**, 1107–1117.
- Wright, S.C., Wei, Q.S., Zhong, J., Zheng, H., Kinder, D.H. & Larrick, J.W. (1994) Purification of a 24-kD protease from apoptotic tumor cells that activates DNA fragmentation. *J. Exp. Med.* **180**, 2113–2123.
- Wu, M., Arsura, M., Bellas, R.E., *et al.* (1996a) Inhibition of *c-myc* expression induces apoptosis of WEHI 231 murine B cells. *Mol. Cell. Biol.* **16**, 5015–5025.
- Wu, M., Lee, H., Bellas, R.E., *et al.* (1996b) Inhibition of NF- $\kappa$ B/Rel induces apoptosis of murine B cells. *EMBO J.* **15**, 4682–4690.
- Yakovlev, A.G., Wang, G., Stoica, B.A., Simbulan-Rosenthal, C.M., Yoshihara, K. & Smulson, M.E. (1999) Role of DNAS1L3 in  $\text{Ca}^{2+}$ - and  $\text{Mg}^{2+}$ -dependent cleavage of DNA into oligonucleosomal and high molecular mass fragments. *Nucleic Acids Res.* **27**, 1999–2005.
- Zhu, H., Dinsdale, D., Alnemri, E.S. & Cohen, G.M. (1997) Apoptosis in human monocytic THP.1 cells involves several distinct targets of N-tosyl-L-phenylalanyl chloromethyl ketone (TPCK). *Cell Death Diff.* **4**, 590–599.

Received: 11 May 2004

Accepted: 23 August 2004